doi: 10.4183/aeb.2023.407

A MODEL TO PREDICT DIAGNOSIS OF PANCREATIC NEUROENDOCRINE TUMORS BASED ON EUS IMAGING FEATURES

I. Saizu[1,3,*], B. Cotruta[1,3], R.A. Iacob[1,3], S. Bunduc[1,3], R.E. Saizu[1,3], M. Dumbrava[2,3], C. Pietrareanu[1,3], G. Becheanu[2,3], D. Grigorie[3,4], C. Gheorghe[1,3]

Clinical Institute Fundeni - [1]Gastroenterology, [2]Pathology, [3]"Carol Davila" University of Medicine and Pharmacy, [4]"C.I. Parhon" National Institute of Endocrinology, Bucharest, Romania

Abstract

Background. This study aimed to determine predictive clinical and endoscopic ultrasound (EUS) features for pancreatic neuroendocrine tumor (PNET) diagnosis, utilizing EUS-guided tissue acquisition.

Methods. A prospective study from 2018-2022 included patients with pancreatic masses undergoing EUS with elastography. Univariate binomial logistic regression followed by multiple logistic regression with significant predictors was employed. A forward selection algorithm identified optimal models based on predictor numbers. Variables encompassed EUS tumor characteristics (e.g., location, size, margins, echogenicity, vascularity on Doppler, main pancreatic duct dilation, elastography appearance, vascular invasion, and hypoechoic rim), alongside demographic and risk factors (smoking, alcohol, diabetes).

Results. We evaluated 165 patients (24 PNETs). EUS features significantly linked with PNET diagnosis were well-defined margins (79% *vs*. 26%, $p < 0.001$), blue elastography appearance (46% *vs*. 9.9%, $p < 0.001$), vascularization (67% *vs*. 25%, $p < 0.001$), hypoechoic rim (46% *vs*. 10%, $p < 0.001$). The top-performing model, with 89.1% accuracy, included two predictors: a homogeneous lesion (OR, 95% CI) and a hypoechoic rim (OR, 95% CI).

Conclusions. EUS appearance can differentiate PNETs from non-PNETs, with the hypoechoic rim being an independent predictor of PNET diagnosis. The most effective predictive model for PNETs combined the homogeneous lesion and presence of the hypoechoic rim.

Keywords: Pancreatic neuroendocrine tumor, Endoscopic ultrasound, Elastography, Hypoechoic rim.

INTRODUCTION

Pancreatic neuroendocrine tumors (PNETs), lately known as islet cell tumors, arise from the endocrine tissue of the pancreas (1). Although uncommon, these lesions seem to have an increasing incidence comprising up to 2% of all pancreatic neoplasias (2-4). These are mainly solid lesions, sometimes harboring a cystic component and based on their ability to secrete hormones, PNTEs are classified as functional and nonfunctional. Nonfunctional tumors are more frequent, representing the majority of up to 75% of all PNETs (5-7).

Size of the lesion, tumor differentiation, tumor invasion of the surrounding structures or blood vessels and the tumor extension to distant organs are considered risk factors of aggressiveness (8, 9). All of these can be determined on routine cross-sectional imaging studies. Nowadays, the sensitivities and specificities of identifying PNETs through CT and MRI vary between 64% to 82% and 74% to 100%, respectively. However, occasionally these can fail to diagnose the primary tumor in 10-20% of cases (10, 11). Moreover, CT scan has difficulties in detecting lesions smaller than 20 mm. In this case, clinical studies found that endoscopic ultrasound (EUS) had a superior sensitivity (overall, 91% *vs.* 63%) (11). Overcoming these limitations, EUS offers additional insights and access to PNETs, enabling it to play a comprehensive role in localizing, staging, confirming, and treating them.

EUS in association with fine needle aspiration (FNA) or fine needle biopsy (FNB) is the standard for pancreatic mass lesions diagnosis (12). There is limited evidence-based data on differentiating neoplastic solid pancreatic lesions, particularly PNETs from solid pancreatic lesions (SPLs) such as pancreatic ductal adenocarcinoma (PDAC) or metastatic lesions to the

*Correspondence to: Ionut Adrian Saizu MD, Clinical Institute Fundeni, Gastroenterology, 258 Fundeni Rd, Bucharest, 022238, Romania, E-mail: saizuadrian@gmail.com

pancreas (PMETs) (10). The goal of this study was to differentiate PNETs from other SPLs by examining specific pretest elements, including risk factors, demographic features, and ultrasound characteristics before cytopathology or histopathology diagnosis. These EUS tumor traits could aid the endoscopist in selecting the needle for performing the tissue acquisition (12).

METHODS

We performed a prospective cohort study at Fundeni Clinical Institute which is a tertiary center of Gastroenterology from Bucharest, Romania, between 2018 and 2022. The study received approval from the hospital's ethics committee and all patients provided written informed consent before undergoing the examination.

Patients' inclusion criteria

EUS with elastography and fine needle aspiration (FNA) were conducted in all patients referred to our department for further evaluation of suspected or diagnosed pancreatic masses based on prior imaging studies of CT scan or MR. All patients with at least one SPL at the time of the diagnosis had to be over 18 years old. The patients selected for the study were those in which EUS-FNA was performed directly from the pancreatic lesion or from adjacent lymphadenopathies). The exclusion criteria were the same as the EUS-FNA contraindications (e.g: coagulation disorders, anticoagulants or anti-platelet therapy, inaccessible lesion by large vessel or pancreatic, biliary duct or metastatic lesion interposition). Furthermore, the patients who refused the study informed consent were not included.

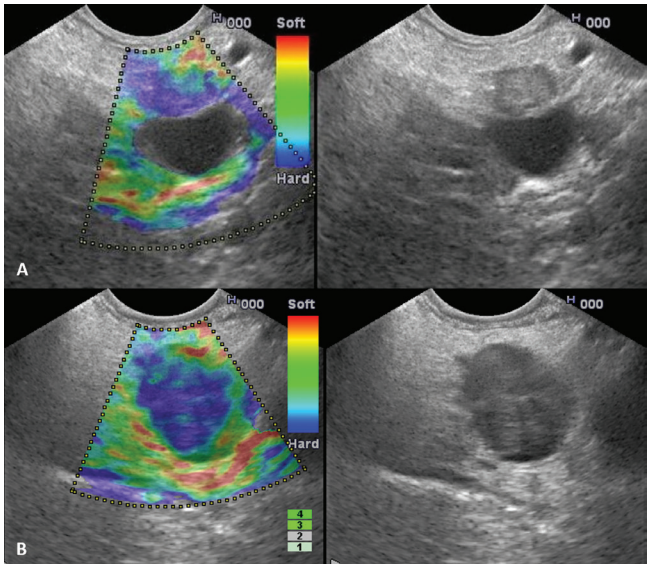

Figure 1. Linear EUS image of a 15 mm well-defined hypoechoic PNET associating a hypoechoic rim, located in the body of the pancreas. The lesion does not invade the splenic vein and there is no PD invasion. During elastography, the tumor does not present a homogenous blue pattern. B. Linear EUS image of a 25 mm well-defined hypoechoic PNET without the presence of the hypoechoic rim. During elastography, the tumor is presenting a homogenous blue pattern.

Procedure

A linear-array ultrasound endoscope was used (EG-3870UTK, Pentax Medical), supporting Real-time Tissue Elastography (RTE) and Doppler function and equipped with a Hitachi Arietta v70 processor or Hitachi EUB-6500HV, Tokyo, Japan. We used either 19 gauge (G), 22G or 25G FNA needles (EchoTip Ultra Endoscopic Ultrasound Needle; Cook Medical, Bloomington, IN, United States). Each procedure was performed by an experienced endoscopist while the patient was under deep sedation with Propofol assisted by an anesthesiologist. There was no need for airway intubation in any of the examined patients. The examining doctor had selected the FNA needle size depending on the location of the lesion and decided the number of needle passes. A cytopathologist was in the endoscopy room conducting an immediate assessment of macroscopic appearance of the aspirate and slides. The procedure concluded upon obtaining an adequate specimen confirmed by both pathologist and endoscopist, respectively. The final diagnosis was established by the histopathological and immunochemistry analysis examination of the FNA (smear, cellblock or paraffin embedded) or subsequently obtained surgical specimen. The case management was performed according to the multidisciplinary tumor board decision.

Variables

The following data were prospectively collected: demographics (i.e., age, sex), personal habits (i.e., smoking and alcohol consumption) and history of diabetes; EUS procedure (i.e., FNA needle size, number of passes), EUS lesion characteristics (i.e., number, location, size (the maximum diameter measured during EUS in millimeters), margins (e.g well-defined or irregular), echogenicity (e.g hypoechoic or not), presence of Doppler signal within the lesion suggesting tumor vascularization, detection of of main pancreatic duct (MPD) dilation (head ≥3.5mm or body ≥2.5mm or tail >1.5mm), the aspect on elastography (e.g homogenous blue pattern or not), detection of

vascular invasion (venous or arterial) and the presence of a hypoechoic rim delineating the interior margins of the lesion (Fig. 1). The EUS tumor characteristics were evaluated by the examining doctor together with a second trainee endoscopist.

Statistical analyses

Except age and tumor size, all the aforementioned data were computed as dichotomous variables. Numerical variables were reported as mean and standard deviation (SD) if normally distributed or median and range. A simple univariate binomial logistic regression was used, the dependent variable being the presence or absence of PNET diagnosis, and the independent variables were the demographic, clinical, and laboratory parameters. Subsequently we performed a multiple logistic regression in which we included the parameters with statistically significant coefficients in the simple logistic regression. A forward selection algorithm generated the best performing models to anticipate the PNET diagnosis for each number of predictors used. P values lower than 0.05 were considered statistically significant. The R program was used for the statistical analysis (version 4.2.3 Copyright (C) 2023 The R Foundation for Statistical Computing, R Core Team 2023). A: A language and environment for statistical computing. R Foundation for Statistical Computing, Vienna, Austria. URL https://www.R-project.org with the following packages: leaps1, cv2, gtsummary3.

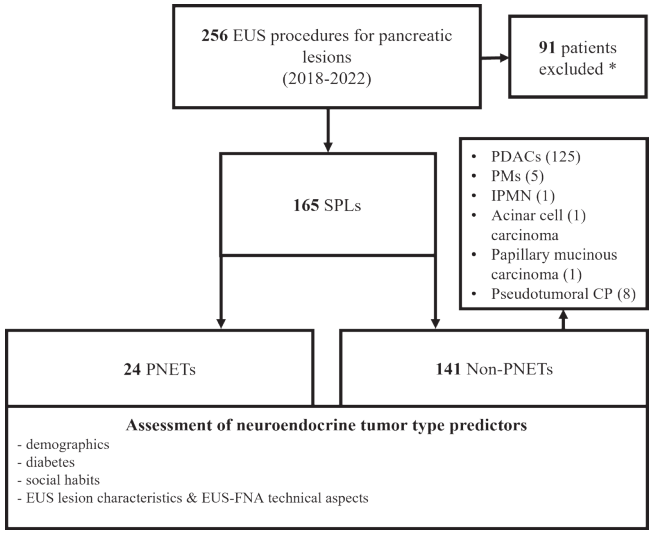

Figure 2. Flowchart depicting selection of study population. EUS FNA – endoscopic ultrasound guided fine needle aspiration; SPLs – solid pancreatic lesions; PDACs – pancreatic ductal adenocarcinomas; PMs – pancreatic metastases; IPMN – intrapapillary mucinous neoplasm; CP- chronic pancreatitis. *Missing data or cystic pancreatic lesions or lack of FNA or lack of informed consent or negative for SPLs.

RESULTS

We are reporting our results based on the STROBE guideline (13). The study flow is represented in Figure 2. Among the patients that were referred for EUS to our department we included in the analysis only those detected with solid lesions. All these patients were diagnosed with pancreatic masses using prior CT or MR imaging studies. Elastography and FNA was performed for all patients included in the study.

All but one patient had FNA from the tumor. In this case, the FNA from the tumor was not possible due to blood vessels interposition. For this reason, the FNA was performed from a lymph node adjacent to the tumor. Out of the total number of patients with pancreatic tumors, the most common diagnoses where pancreatic ductal adenocarcinoma (PDAC) (n= 125) and PNET (n= 24), followed by pancreatic metastases (PM, n= 5), intraductal papillary mucinous neoplasm (IPMN) ductal side branch type (n= 1), acinar cell carcinoma (n= 1) and papillary mucinous carcinoma (n= 1). We evaluated 8 patients as well, previously diagnosed with pseudotumoral chronic pancreatitis, all of them presented negative cytology.

The baseline characteristics of the included patients are detailed in Table 1. The following data was acquired using a simple univariate binomial logistic regression. Among the patients diagnosed with PNET (Table 2), the mean age was 60 years old (±15.0), while non-PNET patients were much older. Sex distribution was even and one third suffered from type 2 diabetes (33%). The majority (80%) were nonsmokers and did not consume alcohol. The median size of the lesions was 37 mm (±16.6) and most of the patients had single pancreatic tumor (88%). Three patients were diagnosed with multiple pancreatic nodules, among which only one had multiple endocrine neoplasia type 1 (MEN-1) incidentally associating a ductal side branch IPMN as a second lesion.

More than half of the PNETs were located in the body of the pancreas (54%) while half of non-PNETs were discovered in the head and only 54 in the body of the pancreas (54% *vs.* 38%, p= 0.03). Main pancreatic duct dilation was seen in 4 patients with PNET (17%). At the same time, almost one third (29%) of the neuroendocrine lesions were presented with vascular invasion. Unexpectedly, half of the patients were found with metastatic disease, which is uncommon for pNETs. Surgical resection of PNET was performed in 8 patients (33%). In 3 cases, surgery confirmed the final diagnosis of PNET, since the FNA results were inconclusive. The

neuroendocrine lesions deemed as unresectable were those with metastatic dissemination.

The EUS features which were significantly associated with the diagnosis of PNET *versus* non-PNET were the well-defined margins of the lesion (79% *vs.* 26%, p< 0.001), the homogeneous lesion (46% *vs.* 9.9%, p< 0.001), the presence of small vessels within the tumor (67% *vs.* 25%, p< 0.001) and the existence of the hypoechoic rim (46% *vs.* 10%, p< 0.001).

Therefore, variables significantly associated with PNE tumor type were used in a multiple logistic regression (Table 3). A forward selection algorithm generated the best performing models for each number of predictors used. The number of predictors varied from 1 to 6 and these were: the homogenous EUS aspect, the well-defined margins, the vascularization, the presence of the hypoechoic rim, the location, and the size of the tumor. The performance of each model was tested using a 10-fold cross-validation procedure. The best performing model obtained was the one with 2 predictors (the homogenous aspect of the lesion and the presence of the hypoechoic rim) with a performance of 89.1%. The influence of the 2 predictors in the analysis model was similar, respectively with OR 6.34 (CI 95% 2.21-18.3) (Table 4). Meanwhile, the model containing all 6 predictors, had a performance of 88%.

Table 1. Baseline characteristics of the included patientsSham Groups

Variables	Total, n= 165
Demographics & history	
Age, mean (SD)	63.55 (11.22)
Sex, n (%)	
F	71 (43)
M	94 (57)
Alcohol, n (%)	58 (35)
Smoker, n (%)	44 (27)
Type 2 diabetes, n (%)	55 (33)
Tumor characteristics	
Tumor location, n (%)	
Head /Uncinate process	78 (47)
Body	67 (41)
Tail	20 (12)
Size (mm), mean (SD)	43.15 (14.40)
MPD dilation, n (%)	31 (19)
Vascular invasion, n (%)	71 (43)
Multiple lesions, n (%)	12 (7.3)
Metastatic disease, n (%)	92 (56)
EUS tumor features	
Well-defined margins, n (%)	53 (32)
Hypoechoic aspect, n (%)	109 (66)
Homogenous aspect, n (%)	25 (15)
Tumor vascularization, n (%)	51 (31)
Blue on elastography, n (%)	123 (75)
Hypoechoic rim, n (%)	25 (15)
EUS FNA	
Needle size, n (%)	
19G	37 (22)
22G	95 (58)
25G	33 (20)
FNA passes, n (%)	
1	57 (35)
2	92 (56)
3	13 (7.9)
4	3 (1.8)
Number of slides, mean (SD)	6.04 (2.70)
***Surgery*, n (%)**	33 (20)

SD, standard deviation; MPD, main pancreatic duct; EUS, endoscopic ultrasound; FNA, fine needle aspiration.

DISCUSSION

In the context of neoplastic SPL, a merger of clinical and paraclinical findings can effectively assist the endosonographer in suggesting a high probability of a PNET lesion prior to cytology or histopathological result. Our study showed that EUS lesion characteristics could predict tumor type in SPLs. Features like well defined margins, vascularization, hypoechoic appearance, and the presence of a hypoechoic rim were significantly associated with PNET diagnosis. Moreover, distal tumor location was significantly more frequent in PNETs as well. On the other hand, demographics, smoking or drinking history, and diabetes diagnosis were not significantly associated with neuroendocrine tumor type. The strongest predictors of PNET in our analysis were the homogenous appearance of the lesion and the presence of a hypoechoic rim.

One meta-analysis evaluating EUS-FNA sensitivity, specificity, and accuracy for detecting SPLs, included 31 studies, more than half of which were retrospective studies and only four of them were performed in multiple centers (14). Our study's noteworthy contribution lies in its prospective design and its uniform patient population, primarily comprising suspicious SPLs. In contrast to patients with non-PNETs, a relative younger patient age indicated a likelihood of PNET diagnosis (mean age: 64.1 years vs. 60 years), aligning with earlier literature data. In a long-term study, evaluating patients older than 35 years old, PNET was the most common malignant tumor diagnosis (15).

The typical aspect of PNET on EUS examination is well known as a hypoechoic, well-delineated, round, homogeneous lesion (11, 16, 17).

In agreement with other reports, the majority of the PNETs evaluated in this study presented these four EUS features. Moreover, less than half of the PNETs associated with the presence of a hypoechoic rim delineating the interior margin of the lesion, making it an independent predictor of neuroendocrine tumor diagnosis. Acoustic shadowing, a reflection artifact stemming from impedance mismatches or refraction at tissue boundaries, leads to a hyperechoic signal at interfaces, creating a shadow effect where echo signals are absent. This phenomenon aids in diagnosing conditions such as biliary and pancreatic stones or calcifications in the pancreas. Furthermore, acoustic shadowing can also be caused by refraction at a boundary between tissues with different acoustic velocities, especially if the margin is curved (e.g., mostly in cystic lesions or tumors). Refraction, occurring when the angle of incidence is not normal to the delineation between the tissues, redirects the ultrasound beam, creating an acoustic shadow in certain tissue regions. The result in the ultrasound image is the hypoechoic rim that outlines the interior margin of the tumor (Fig. 1) (18, 19).

The commonly employed criteria in predicting

Table 2. Comparative analysis of PNET lesions *vs.* non-PNETs (PDAC, PM, IPMN, acinar cell carcinoma and papillary mucinous carcinoma)

Variable	non-PNET, n= 141 (%)	PNET, n= 24 (%)	p-value[1]
Demographics			
Age, mean (SD)	64.15 (10.4)	60.0 (15.0)	0.20
Females, n (%)	59 (42)	12 (50)	0.46
Personal history and habits			
Alcohol, n (%)	53 (38)	5 (21)	0.11
Smoker, n (%)	40 (28)	4 (17)	0.23
Type II Diabetes, n (%)	47 (33)	8 (33)	0.99
Tumor characteristics			
Location, n (%)			0.036
Head /Uncinate process	72 (51)	6 (25)	
Body	54 (38)	13 (54)	
Tail	15 (11)	5 (21)	
Mean size (mm) (SD)	44.07 (13.84)	37.71 (16.62)	0.087
MPD dilation, n (%)	27 (19)	4 (17)	0.99
Vascular invasion, n (%)	64 (45)	7 (29)	0.14
Multiple lesions, n (%)	9 (6.4)	3 (13)	0.39
Metastatic disease, n (%)	81 (58)	11 (46)	0.26
EUS tumor features			
Well-defined margins, n (%)	36 (26)	17 (71)	<0.001
Hypoechoic aspect, n (%)	90 (64)	19 (79)	0.14
Homogenous aspect, n (%)	14 (9.9)	11 (46)	<0.001
Tumor vascularization, n (%)	35 (25)	16 (67)	<0.001
Blue on elastography, n (%)	105 (74)	18 (75)	0.96
Hypoechoic rim, n (%)	14 (9.9)	11 (46)	<0.001
EUS FNA			
Needle size, n (%)			0.008
19G	28 (20)	9 (38)	
22G	88 (62)	7 (29)	
25G	25 (18)	8 (33)	
FNA passes, n (%)			0.99
1	49 (35)	8 (33)	
2	78 (55)	14 (58)	
3	11 (7.8)	2 (8.3)	
4	3 (2.1)	0 (0)	
Smears, Mean (SD)	6.14 (2.69)	5.46 (2.70)	0.26
Tumor differentiation			
G1	-	4 (16.6)	-
G2	-	4 (16.6)	-
G3	-	16 (66.6)	-

PNET, pancreatic neuroendocrine tumor; PDAC, pancreatic ductal adenocarcinoma; PM, pancreatic metastases; IPMN, intraductal papillary mucinous cancer; SD, standard deviation; MPD, main pancreatic duct; EUS, endoscopic ultrasound; FNA, fine needle aspiration. 1 Welch Two Sample t-test; Pearson's Chi-squared test; Fisher's exact test.

Table 3. Simple univariate binomial logistic regression of risk factors, and EUS features comparing PNET and non-PNET SPLs

Predictor Variable	Total patients, n	PNET, n	OR (95% CI) *	p-value
Demographics, personal history, and habits				
Sex (male)	94	12	0.72 (0.30 to 1.73)	0.457
Alcohol	58	5	0.44 (0.14 to 1.16)	0.120
Smoker	44	4	0.51 (0.14 to 1.44)	0.238
Type II Diabetes	55	8	1.00 (0.38 to 2.45)	0.999
Tumor characteristics				
Tumor location				
Head /Uncinate process	78	6	—	
Body	67	13	2.89 (1.07 to 8.68)	0.043
Tail	20	5	4.00 (1.04 to 15.1)	0.038
MPD dilation	31	4	0.84 (0.23 to 2.46)	0.774
Vascular invasion	71	7	0.50 (0.18 to 1.23)	0.143
Multiple lesions	12	3	2.08 (0.44 to 7.64)	0.300
EUS tumor features				
Well-defined margins	53	17	7.08 (2.82 to 19.6)	<0.001
Hypoechoic aspect	109	19	2.15 (0.81 to 6.80)	0.150
Homogenous aspect	25	11	7.68 (2.89 to 20.6)	<0.001
Tumor vascularization	51	16	6.06 (2.45 to 16.1)	<0.001
Blue on elastography	123	18	1.03 (0.40 to 3.02)	0.956
Hypoechoic rim	25	11	7.68 (2.89 to 20.6)	<0.001

PNET, pancreatic neuroendocrine tumor; SD, standard deviation; MPD, main pancreatic duct; EUS, endoscopic ultrasound.* OR - Odds Ratio, CI - Confidence Interval.

Table 4. The influence of the 2 predictors in the best performing model – 89.1% performance

Predictor	OR (95% CI) *	p-value
Homogenous aspect	6.34 (2.21 to 18.3)	<0.001
Hypoechoic rim	6.34 (2.21 to 18.3)	<0.001

* OR - Odds Ratio; CI - Confidence Interval.

PNETs behavior include size or changes in size over time, morphological appearance, grade, and expression of Ki-67 (16, 20). The present study had a great variation regarding the PNETs size range (from 10 mm to 70 mm) suggesting the heterogeneity of this type of tumors. More than two thirds of patients were diagnosed with PNET had high grade tumors (G3). Furthermore, as mentioned before, half of all PNETs were considered cancers because of the presence of metastases, two thirds having unresectable disease which is in contradiction with other studies (21). This discrepancy might be explained by the paucity of EUS availability in secondary medical centers and by the steep learning curve of EUS technique (12, 22, 23). In addition, imaging evidence of vascular invasion indicates a poor prognostic but PNETs typically do not exhibit this trait mostly seen in PDACs (24, 25). Out of the few neuroendocrine tumors with vascular invasion, the majority were larger than 40 mm and only two were associated with pancreatic duct dilation. Compared with pancreatic adenocarcinomas, which most are located in the head of the pancreas and are linked to PD dilation, PNETs can present with a more indolent course (24, 25). Half of the evaluated patients diagnosed with this type of tumor, presented with lesions found in the body of the pancreas hence did not exhibit PD dilation.

The relationship between tobacco smoke, alcohol, diabetes and PDAC is well known, with 20-30% of cases attributed to smoking. Furthermore, exposure to environmental tobacco smoke, particularly during childhood and *in-utero* heightens this risk as well (26-29). Although cigarette smoking, alcohol consumption and newly onset diabetes diagnosis are strongly associated with PDAC, these were observed only in a small fraction of patients diagnosed with PNET.

Elastography assesses the elasticity or firmness of a particular tissue in comparison to adjacent normal tissue and it can be conducted qualitatively or quantitatively. Qualitative assessment is limited by its subjective nature and relies mainly on color patterns and the uniformity of color distribution. A meta-analysis by Mei *et al.* involving 1,044 patients, focused on qualitative EUS elastography for diagnosing SPLs, demonstrating a high sensitivity of 95% but a relatively low specificity of 67% (30). As expected, in the current study, 75% of the PNET lesions expressed a homogenous blue aspect on elastographic evaluation, nearly the same as non-PNETs. This feature did not statistically correlate with the diagnosis of neuroendocrine tumor. In contrast, quantitative elastography offers an objective means of measuring tissue hardness through the computation of the strain

ratio (SR), where a higher SR indicates decreased elasticity. Its superiority is proven in a study performed by Iglesias García *et al*. who found a sensitivity of 100% and specificity of 88% when using quantitative elastography to distinguish pancreatic adenocarcinoma from PNETs, with a cutoff value of SR set at 26.6 (31).

Despite current trend of switching to fine needle biopsy (FNB), European Society of Gastrointestinal Endoscopy (ESGE), equally recommends the use of 25G/22G FNA or FNB needles for routine EUS-guided sampling of solid masses and lymph nodes (LNs). However, when the primary goal is to acquire a core tissue specimen, ESGE recommends utilizing 19G FNA or FNB needles, or a 22G FNB needle (12). During examination, the endoscopist had discretion in selecting the FNA needle size depending on tumor location. The number of needle passes was decided after an on-site macroscopic examination of the sample performed by the endosonographer and cytopathologist as well. The most used needle in diagnosing non-PNETs was the 22G FNA needle (60%). On the other hand, all three needle sizes were used equally for the diagnosis of the PNETs with a slight predominance of the 19G needle (p= 0.008). An explanation would be the larger diameter of the needle, which would have the ability to sample more tumor tissue (12). In contrast, evidence-based data showed 19G needles are cumbersome to use compared to 22G needles in sampling SPLs found in the head of the pancreas, with no differences in tissue acquisition (32, 33).

Study limitations

There are some important limitations of the study worth mentioning. Despite being a prospective observational study, this is a single-center analysis performed in a tertiary hospital specialized in hepatobiliopancreatic diseases and the outcomes might not necessarily mirror the practices employed in different medical centers. Elastographic quantitative assessment of the lesions would have added an objective side to the analysis by avoiding defining subjective color patterns. On the other hand, artificial intelligence (AI), might have a role in eliminating this biased issue with the help of AI-assisted EUS image analysis models. A meta-analysis, using newer AI models of EUS elastography demonstrated a sensitivity and a specificity of 98% and 63% respectively for diagnosing malignant pancreatic lesions. In the future, this could serve as a valuable complementary approach to EUS-FNA for distinguishing pancreatic masses (34). The lack of using contrast enhanced EUS (CEUS) in evaluating the SPLs certainly is a drawback of the study. There are important data in literature of CEUS alone or in association with elastography in showing its importance in differentiating SPLs (35). Another aspect which might not certainly reflect real-life encounters is that the examined lesions were exclusively SPL. This was chosen in order to assess EUS characterization. The detection of pancreatic cystic lesions is rising hence the incidence of PNET associated with cystic component. For this reason, when a pancreatic cystic lesion is detected, it is crucial to be properly characterized in order to differentiate the neoplastic from non-neoplastic aspect (36).

In conclusion, EUS appearance can suggest the diagnosis of PNET. The presence of a hypoechoic rim delimiting the interior margin of the lesion is an independent predictor of the diagnosis. Moreover, in the multivariate analysis the best performing model in predicting PNETs was the association of the homogenous aspect of the lesion and the presence of the hypoechoic rim. During EUS for solid homogenous pancreatic masses, the presence of this rim should encourage the endoscopists to use a 19G FNA needle or switch to FNB needle in order acquire a core tissue specimen adequate for further immunohistochemical analysis.

Conflict of interest

The authors declare that they have no conflict of interest.

Acknowledgements

This work was supported by the European Research Executive Agency under the project Training in translational protocols for minimal invasive diagnosis and therapy in pancreatico-biliary cancers – TRIP (grant agreement number: 101079210).

Data sharing statement

The data underlying this article will be shared upon reasonable request to the corresponding author.

References

1. Reznek R. Islet cell tumours. Cancer Imaging. 2003;4(1):1-4.
2. Klimstra DS. Nonductal neoplasms of the pancreas. Mod Pathol 2007; 20 Suppl 1: S94.
3. Hallet J, Law CH, Cukier M, Saskin R, Liu N, Singh S. Exploring the rising incidence of neuroendocrine tumors: a population-based analysis of epidemiology, metastatic presentation, and outcomes. Cancer. 2015;121(4):589-597.
4. Dasari A, Shen C, Halperin D, Zhao B, Zhou S, Xu Y, Shih T, Yao JC. Trends in the Incidence, Prevalence, and Survival Outcomes in Patients with Neuroendocrine Tumors in the United States. JAMA Oncol. 2017; 3:1335-1342.
5. Ito T, Tanaka M, Sasano H, Osamura YR, Sasaki I, Kimura W, Takano K, Obara T, Ishibashi M, Nakao K, Doi R, Shimatsu A,

Nishida T, Komoto I, Hirata Y, Imamura M, Kawabe K, Nakamura K; Neuroendocrine Tumor Workshop of Japan. Preliminary results of a Japanese nationwide survey of neuroendocrine gastrointestinal tumors. J Gastroenterol. 2007; 42(6):497-500.
6. Badan MI, Piciu D. Immunohistochemical markers and SPECT/CT somatostatin-receptor (99mtc-Tektrotyd) uptake in well and moderately differentiated neuroendocrine tumors. Acta Endocrinol (Buchar). 2022;18(4):523-530.
7. Badiu C Neuroendocrine tumors: review of pathology, molecular and therapeutic advances. Acta Endocrinol (Buchar). 2018;14(1):145.
8. Imamura M. Recent standardization of treatment strategy for pancreatic neuroendocrine tumors. World J Gastroenterol. 2010;16(36):4519-4525.
9. Kloppel G, Rindi G, Perren A, Komminoth P, Klimstra DS. The ENETS and AJCC/UICC TNM classifications of the neuroendocrine tumors of the gastrointestinal tract and the pancreas à statement. Virchow Arch. 2010; 456(6):595-597.
10. Gagovic V, Spier BJ, DeLee RJ, Barancin C, Lindstrom M, Einstein M, Byrne S, Harter J, Agni R, Pfau PR, Frick TJ, Soni A, Gopal DV. Endoscopic ultrasound fine-needle aspiration characteristics of primary adenocarcinoma versus other malignant neoplasms of the pancreas. Can J Gastroenterol. 2012;26(10):691-696.
11. Khashab MA, Yong E, Lennon AM, Shin EJ, Amateau S, Hruban RH, Olino K, Giday S, Fishman EK, Wolfgang CL, Edil BH, Makary M, Canto MI. EUS is still superior to multidetector computerized tomography for detection of pancreatic neuroendocrine tumors. Gastrointest Endosc. 2011;73(4):691-696.
12. Polkowski M, Jenssen C, Kaye P, Carrara S, Deprez P, Gines A, Fernández-Esparrach G, Eisendrath P, Aithal GP, Arcidiacono P, Barthet M, Bastos P, Fornelli A, Napoleon B, Iglesias-Garcia J, Seicean A, Larghi A, Hassan C, van Hooft JE, Dumonceau JM. Technical aspects of endoscopic ultrasound (EUS)-guided sampling in gastroenterology: European Society of Gastrointestinal Endoscopy (ESGE) Technical Guideline - March 2017. Endoscopy. 2017;49(10):989-1006.
13. Cuschieri S. The STROBE guidelines. Saudi J Anaesth. 2019; 13(Suppl 1): S31-S34.
14. Chen G, Liu S, Zhao Y, Dai M, Zhang T. Diagnostic accuracy of endoscopic ultrasound-guided fine-needle aspiration for pancreatic cancer: a meta-analysis. Pancreatology. 2013;13(3):298-304.
15. Redelman M, Cramer HM, Wu HH. Pancreatic fine-needle aspiration cytology in patients < 35-years of age: a retrospective review of 174 cases spanning a 17-year period. Diagn Cytopathol. 2014;42(4):297-301.
16. Figueiredo FA, Giovannini M, Monges G, Charfi S, Bories E, Pesenti C, Caillol F, Delpero JR. Pancreatic endocrine tumors: a large single-center experience. Pancreas. 2009;38(8):936-940.
17. Krishna SG, Bhattacharya A, Li F, Ross WA, Ladha H, Porter K, Atiq M, Bhutani MS, Lee JH. Diagnostic Differentiation of Pancreatic Neuroendocrine Tumor from Other Neoplastic Solid Pancreatic Lesions During Endoscopic Ultrasound-Guided Fine-Needle Aspiration. Pancreas. 2016;45(3):394-400.
18. Steel R, Poepping TL, Thompson RS, Macaskill C. Origins of the edge shadowing artifact in medical ultrasound imaging. Ultrasound Med Biol. 2004; 30(9):1153-1162. Erratum in: Ultrasound Med Biol. 2005;31(1):135.
19. Rubin JM, Adler RS, Fowlkes JB, Carson PL. Phase cancellation: a cause of acoustical shadowing at the edges of curved surfaces in B-mode ultrasound images. Ultrasound Med Biol. 1991;17(1):85-95.
20. Bartolini I, Bencini L, Risaliti M, Ringressi MN, Moraldi L, Taddei A. Current Management of Pancreatic Neuroendocrine Tumors: From Demolitive Surgery to Observation. Gastroenterol Res Pract. 2018;2018:9647247.
21. Lawrence B, Gustafsson BI, Chan A, Svejda B, Kidd M, Modlin IM. The epidemiology of gastroenteropancreatic neuroendocrine tumors. Endocrinol Metab Clin North Am. 2011;40(1):1-18, vii.
22. Polkowski M, Larghi A, Weynand B, Boustière C, Giovannini M, Pujol B, Dumonceau JM; European Society of Gastrointestinal Endoscopy (ESGE). Learning, techniques, and complications of endoscopic ultrasound (EUS)-guided sampling in gastroenterology: European Society of Gastrointestinal Endoscopy (ESGE) Technical Guideline. Endoscopy. 2012;44(2):190-206.
23. Johnson G, Webster G, Boškoski I, Campos S, Gölder SK, Schlag C, Anderloni A, Arnelo U, Badaoui A, Bekkali N, Christodoulou D, Czakó L, Fernandez Y Viesca M, Hritz I, Hucl T, Kalaitzakis E, Kylänpää L, Nedoluzhko I, Petrone MC, Poley JW, Seicean A, Vila J, Arvanitakis M, Dinis-Ribeiro M, Ponchon T, Bisschops R. Curriculum for ERCP and endoscopic ultrasound training in Europe: European Society of Gastrointestinal Endoscopy (ESGE) Position Statement. Endoscopy. 2021;53(10):1071-1087.
24. Oberg K, Eriksson B. Endocrine tumours of the pancreas. Best Pract Res Clin Gastroenterol. 2005; 19:753–781.
25. Adsay NV, Andea A, Basturk O, Kilinc N, Nassar H, Cheng JD. Secondary tumors of the pancreas: an analysis of a surgical and autopsy database and review of the literature. Virchows Arch. 2004;444(6):527-535.
26. Lowenfels AB, Maisonneuve P. Epidemiology and risk factors for pancreatic cancer. Best Pract Res ClinGastroenterol. 2006; 20:197-209.
27. Vrieling A, Bueno-de-Mesquita HB, Boshuizen HC, Michaud DS, Severinsen MT, Overvad K, Olsen A, Tjønneland A, Clavel-Chapelon F, Boutron-Ruault MC, Kaaks R, Rohrmann S, Boeing H, Nöthlings U, Trichopoulou A, Moutsiou E, Dilis V, Palli D, Krogh V, Panico S, Tumino R, Vineis P, van Gils CH, Peeters PH, Lund E, Gram IT, Rodríguez L, Agudo A, Larrañaga N, Sánchez MJ, Navarro C, Barricarte A, Manjer J, Lindkvist B, Sund M, Ye W, Bingham S, Khaw KT, Roddam A, Key T, Boffetta P, Duell EJ, Jenab M, Gallo V, Riboli E. Cigarette smoking, environmental tobacco smoke exposure and pancreatic cancer risk in the European Prospective Investigation into Cancer and Nutrition. Int J Cancer. 2010; 126:2394.
28. Bao Y, Giovannucci E, Fuchs CS, Michaud DS. Passive smoking and pancreatic cancer in women: a prospective cohort study. Cancer Epidemiol Biomarkers Prev. 2009; 18:2292.
29. Cuzick J, Babiker AG. Pancreatic cancer, alcohol, diabetes mellitus and gall-bladder disease. Int J Cancer. 1989; 43:415–21.
30. Mei M, Ni J, Liu D, Jin P, Sun L. EUS elastography for diagnosis of solid pancreatic masses: a meta-analysis. Gastrointest Endosc. 2013;77(4):578-589.
31. Iglesias-Garcia J, Larino-Noia J, Abdulkader I, Forteza J, Dominguez-Munoz JE. Quantitative endoscopic ultrasound elastography: an accurate method for the differentiation of solid pancreatic masses. Gastroenterology. 2010;139(4):1172-1180.
32. Facciorusso A, Wani S, Triantafyllou K, Tziatzios G, Cannizzaro R, Muscatiello N, Singh S. Comparative accuracy of needle sizes and designs for EUS tissue sampling of solid pancreatic masses: a network meta-analysis. Gastrointest Endosc. 2019;90(6): 893-903.e7.
33. Laquière A, Lefort C, Maire F, Aubert A, Gincul R, Prat F, Grandval P, Croizet O, Boulant J, Vanbiervliet G, Pénaranda G, Lecomte L, Napoléon B, Boustière C. 19 G nitinol needle versus 22 G needle for transduodenal endoscopic ultrasound-guided sampling of pancreatic solid masses: a randomized study. Endoscopy. 2019; 51(5): 436-443.
34. Zhang B, Zhu F, Li P, Yu S, Zhao Y, Li M. Endoscopic ultrasound elastography in the diagnosis of pancreatic masses: A meta-analysis. Pancreatology. 2018;18(7):833-840.
35. Iglesias-Garcia J, Lindkvist B, Lariño-Noia J, Abdulkader-Nallib I, Dominguez-Muñoz JE. Differential diagnosis of solid pancreatic masses: contrast-enhanced harmonic (CEH-EUS), quantitative-elastography (QE-EUS), or both? United European Gastroenterology Journal. 2017;5(2):236-246.
36. Kongkam P, Al-Haddad M, Attasaranya S, O'Neil J, Pais S, Sherman S, DeWitt J. EUS and clinical characteristics of cystic pancreatic neuroendocrine tumors. Endoscopy. 2008;40(7):602-605.